

# $\Sigma^-/\Sigma^+$ ratio as a candidate for probing the density dependence of the symmetry potential at high nuclear densities

Qingfeng LI<sup>1,4)</sup>, Zhuxia LI<sup>2,1,3,4)</sup>, Enguang ZHAO<sup>4)</sup> and Raj K. GUPTA<sup>1,5)</sup>

1) *Frankfurt Institute for Advanced Studies (FIAS),*

*Johann Wolfgang Goethe-Universität, Max-von-Laue-Str. 1,*

*D-60438 Frankfurt am Main, Germany*

2) *China Institute of Atomic Energy,*

*P. O. Box 275 (18), Beijing 102413, P. R. China*

3) *Center of Theoretical Nuclear Physics,*

*National Laboratory of Lanzhou Heavy Ion Accelerator, Lanzhou 730000, P. R. China*

4) *Institute of Theoretical Physics, Chinese Academy of Sciences,*

*P. O. Box 2735, Beijing 100080, P. R. China*

5) *Department of Physics, Panjab University, Chandigarh - 160014, India*

## Abstract

Based on the UrQMD model, we have investigated the influence of the symmetry potential on the negatively and positively charged  $\pi$  and  $\Sigma$  hyperon production ratios in heavy ion collisions at the SIS energies. We find that, in addition to  $\pi^-/\pi^+$  ratio, the  $\Sigma^-/\Sigma^+$  ratio can be taken as a sensitive probe for investigating the density dependence of the symmetry potential of nuclear matter at high densities (1-4 times of normal baryon density). This sensitivity of the symmetry potential to both the  $\pi^-/\pi^+$  and  $\Sigma^-/\Sigma^+$  ratios is found to depend strongly on the incident beam energy. Furthermore, the  $\Sigma^-/\Sigma^+$  ratio is shown to carry the information about the isospin-dependent part of the  $\Sigma$  hyperon single-particle potential.

PACS numbers: 24.10.Lx, 25.75.Dw, 25.75.-q

## I. INTRODUCTION

The equation of state (EoS) has attracted a lot of attention recently for asymmetric nuclear matter, which can be described approximately by the parabolic law

$$e(\rho, \delta) = e_0(\rho, 0) + e_{sym}(\rho)\delta^2. \quad (1)$$

Here  $\delta = (\rho_n - \rho_p)/(\rho_n + \rho_p)$  is the isospin asymmetry,  $e_0$  the energy per nucleon for symmetric nuclear matter, and  $e_{sym}(\rho)$  the bulk symmetry energy. The symmetry energy term  $e_{sym}(\rho)\delta^2$  is very important for understanding many interesting astrophysical phenomena (see, *e.g.* [1]), but so far results in large uncertainties: *e.g.*, the symmetry energy calculated with different kinds of parameter sets (Skyrme or Gogny type) are largely divergent [2, 3]), especially at high densities, and for some cases, *i.e.*, when the density is higher than three times of the normal density, even a negative symmetry energy can be obtained. Therefore, acquiring the more accurate knowledge of the symmetry energy, and the isospin asymmetry, becomes one of the main goals in nuclear physics at present. The recently available facilities of rare-isotope beams provide the opportunities to study the dynamical evolution of nuclear systems with a large range of isospin asymmetries, which increases the domain over which a spatially uniform local isospin asymmetry  $\delta(r)$  may be achieved.

In order to obtain the information about the symmetry potential at high density, the beam energy required has to be of higher than several hundreds of MeV per nucleon, but then the isospin effects on heavy ion collisions would become negligible and are usually not considered. However, in some special cases, like the one around the particle emission threshold, it is found that the symmetry potential affects the particle production [4, 5, 6, 7], especially, the ratio between the number of produced negatively and positively charged particles may depend sensitively on the density dependence of the symmetry potential. B.A. Li [8, 9] found that, in an isospin-dependent hadronic transport model, the  $\pi^-/\pi^+$  ratio, as well as the neutron-proton differential collective flow, were sensitive to the behavior of the nuclear symmetry potential at high densities. More recently, within the framework of relativistic Landau Vlasov transport method, Gaitanos et al. [10, 11] found that when the beam energy was higher than 2 AGeV the sensitivity of  $\pi^-/\pi^+$  ratio to the form of the symmetry potential is largely reduced at high densities. In this paper, we attempt a further investigation of the energy dependence of the sensitivity of the  $\pi^-/\pi^+$  production ratio to the form of the symmetry potential in the UrQMD model. Furthermore, we try to explore

a new candidate in terms of the  $\Sigma^-/\Sigma^+$  ratio for probing the symmetry potential in high density matter, which is in addition to the  $\pi^-/\pi^+$  production ratio.

The production of  $\Sigma^-$  and  $\Sigma^+$  hyperons is closely related to the neutron-proton asymmetry of the projectile-target system, which means that the symmetry potential of nuclear matter will affect the  $\Sigma^-/\Sigma^+$  ratio. Consequently, the  $\Sigma^-/\Sigma^+$  ratio in heavy ion collisions at high energies may also carry the information about the density dependence of the symmetry potential of nuclear matter. Furthermore, the isospin-dependent part of the single-particle potential of  $\Sigma$  hyperon in a nuclear medium, the, so called, Lane potential, depends on the isospin asymmetry of nuclear matter, which might also influence the  $\Sigma^-/\Sigma^+$  ratio. In turn, this study of  $\Sigma^-/\Sigma^+$  ratio might provide us with the information about the isospin-dependent part of the  $\Sigma$  hyperon single-particle potential.

In this paper, the study of  $\Sigma$  hyperon production is limited near its threshold (1.79 GeV for  $\Sigma$  hyperon production in free space through a process of the type  $BB \rightarrow BKY$  reaction) in order to observe the effect of the symmetry potential on the  $\Sigma^-/\Sigma^+$  ratio. Specifically, we consider the neutron-rich system  $^{132}\text{Sn} + ^{132}\text{Sn}$  and the nearly isospin-symmetric system  $^{112}\text{Sn} + ^{112}\text{Sn}$  at three different beam energies of  $1.5A$  (the sub-threshold energy),  $2.5A$ , and  $3.5A$  GeV. For our calculations, the UrQMD model [12, 13, 14, 15], version 1.3, is adopted, using the 'hard' Skyrme-type EoS for reactions with beam energies  $E_b \leq 4A$  GeV. We find that most of the UrQMD model calculations can simultaneously reproduce many experimental measurements, which offers a good platform for studying the isospin effects at SIS energies.

The paper is arranged as follows. In section II, we give our method of including the isospin-dependent part of the mean field in the UrQMD transport model. In section III, the numerical results of pion and  $\Sigma$  hyperon production and the corresponding ratios between the negatively and positively charged particles are presented. Finally, in section IV, a brief summary and discussion are given.

## II. THE TREATMENT OF THE ISOSPIN-DEPENDENT PART OF THE MEAN FIELD IN THE URQMD MODEL

Since the isospin dependence of nucleon-nucleon interaction has been introduced explicitly in the UrQMD model, in order to study the isospin effects in heavy ion collisions, we have to

introduce the symmetry potential into the mean field. In UrQMD model, the Skyrme and the Yukawa potentials are included in the iso-scalar part of the mean field, where the Yukawa parameter is related to Skyrme parameters. In infinite nuclear matter, the contribution of Yukawa potential to the total energy acts like the two-body Skyrme contribution [12]. The Coulomb potential is also implemented explicitly. Similarly, a symmetry potential should also be included in the mean-field part.

The bulk symmetry energy  $e_{sym}$  in Eq. (1) can be expressed as

$$e_{sym} = S_0 F(u), \quad (2)$$

where  $S_0$  is the symmetry energy at the normal density and  $u = \rho/\rho_0$  the reduced density. In this paper, we take  $S_0 = 30$  MeV and, in order to mimic the strong variation of the density dependence of the symmetry energy at high densities, we adopt the form of  $F(u)$  as used in [8]:

$$F(u) = \begin{cases} F_1 = u^\gamma & \gamma > 0 \\ F_2 = u \cdot \frac{a-u}{a-1} & a > 1 \end{cases}. \quad (3)$$

Here  $a$  is the reduced critical density. Note that when  $u > a$ , the symmetry potential energy will be negative. Similarly, following [8], we take  $\gamma = 1$  for stiff symmetry potential (stiff-sym.pot.), namely, the  $F_1^{\gamma=1}$ , and  $a = 3$  for soft symmetry potential (soft-sym.pot.), namely, the  $F_2^{a=3}$ . Apparently,  $F_1^{\gamma=1}$  and  $F_2^{a=3}$  give the two extremes of the symmetry energy at high densities, as is illustrated in the following for the chemical potential.

The neutron and proton chemical potentials  $\mu_{n/p}^{sym}$ , contributed only by the symmetry potential energy, are shown in Fig. 1. We notice in Fig. 1 that for  $u < 1$  the difference between the neutron (and so also proton) chemical potentials calculated with  $F_1^{\gamma=1}$  and  $F_2^{a=3}$  is small but becomes large at high densities. For  $u > 2.6$ , the  $\mu_n^{sym}$  becomes negative for  $F_2^{a=3}$ . Furthermore, the curves of  $\mu_n^{sym}$  for  $F_1^{\gamma=1}$  and  $F_2^{a=3}$  cross each other at  $u \sim 0.8$  (called, crossing point) and those of  $\mu_p^{sym}$  at  $u \sim 1.1$ . Apparently, such different behaviors of the  $\mu_{n/p}^{sym}$ , calculated with  $F_1^{\gamma=1}$  and  $F_2^{a=3}$ , will strongly influence the motion of protons and neutrons and so also the time evolution of the proton and neutron density distributions, which will further influence the ratios of produced particles with different charges.

For simplicity, the isospin-independent part of the mean field for resonances and hyperons is taken here to be the same as that of the nucleon. This simplification is quite adventurous, but we think that it should not alter the final conclusion about the influence of the

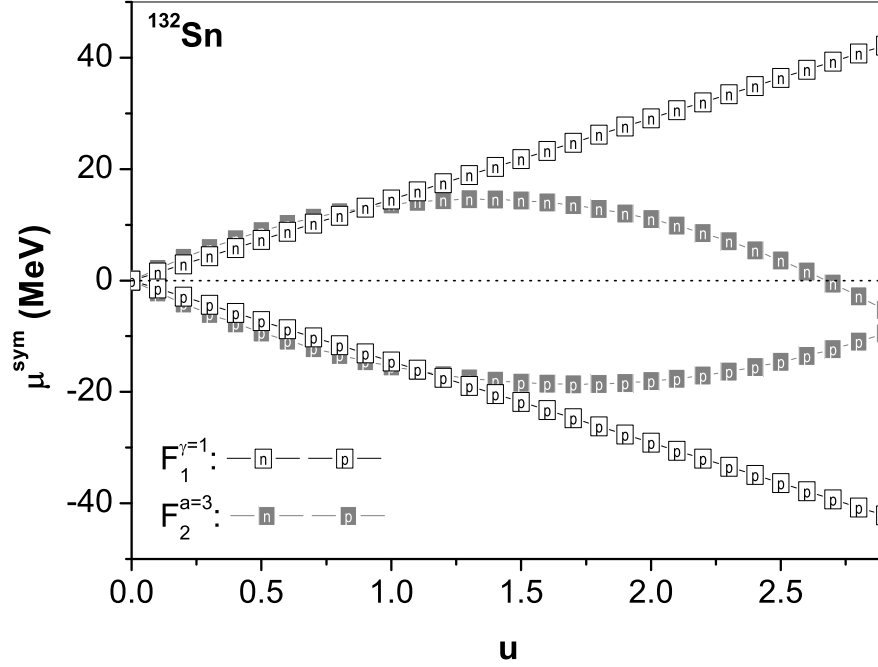


FIG. 1: The neutron and proton chemical potentials, contributed only by the symmetry potential energy, calculated for  $^{132}\text{Sn}$ , using both the stiff-sym.pot.  $F_1^{\gamma=1}$  and soft-sym.pot.  $F_2^{a=3}$ . Here  $\delta = (82 - 50)/132$ .

symmetry potential on the ratios of emitted negatively versus positively charged particles. The symmetry potentials of the resonances [ $N^*(1440)$  and  $\Delta(1232)$ ] and hyperons [ $\Lambda$  and  $\Sigma$ ] are also introduced in the calculations, in addition to that of the nucleon. The symmetry potential for the resonances is obtained through the constants of isospin coupling (the Clebsch-Gordan coefficients) in the process of  $\Delta(1232)$  [or  $N^*(1440)$ ]  $\leftrightarrow \pi N$ .

For hyperons, the single-particle potential in a spin-saturated nuclear matter can be expressed as

$$V_{\Sigma\pm} = V_0 \mp \frac{1}{2}V_1\delta, \quad (4)$$

assuming charge independence of the baryon-baryon interaction [16, 17]. Here  $V_0$  and  $V_1$  represent the isospin-independent and -dependent parts. The  $V_1$  is the Lane potential, which is known to be important for the structure of the  $\Sigma$  hyper-nuclear state[18, 19]. This expression has the same form as the single-particle potential of nucleons, up to the first order in  $\delta$ . However, the value of  $V_1$ , even its sign, is still a matter of argument: within

TABLE I: The values of  $\alpha$  and  $\beta$  for isospin-dependent potentials of different baryons.

B	$\alpha$	$\beta$	B	$\alpha$	$\beta$
$N^{*0}(1440)$	1/3	2/3	$\Lambda$	1/2	1/2
$N^{*+}(1440)$	2/3	1/3	$\Delta^-$	1	0
$\Sigma^-$	1	0	$\Delta^0$	2/3	1/3
$\Sigma^0$	1/2	1/2	$\Delta^+$	1/3	2/3
$\Sigma^+$	0	1	$\Delta^{++}$	0	1

the relativistic mean-field theory (see, *e.g.*, [20, 21]), the symmetry potential of the octet of baryons is described via the coupling between the baryon and  $\rho$  meson. For hyperons ( $H$ ), the isospin dependent part is determined by the coupling constant  $g_{H\rho}$  and their isospin. Since  $g_{H\rho}$  is taken to be  $< g_{N\rho}$ , as well as  $> g_{N\rho}$  [20], we simply take the symmetry potential of  $\Sigma^\pm$  hyperon to be proton-like and neutron-like, according to Eq. (4). However, the symmetry potential of the excited states of hyperon is not considered, for lack of information.

Combining both the resonances and hyperons, we express the symmetry potential in an unified form, which reads as

$$v_{sym}^B = \alpha v_{sym}^n + \beta v_{sym}^p, \quad (5)$$

where the values of  $\alpha$  and  $\beta$  for different baryons ( $B$ ) are listed in Table I. From this table we can see that the symmetry potentials of  $\Delta^-$  and  $\Sigma^-$  are neutron-like and those of  $\Delta^{++}$  and  $\Sigma^+$  are proton-like. On the other hand, the symmetry potentials of  $\Delta^0$ ,  $\Delta^+$  and  $N^*(1440)$  are a mixture of the neutron and proton symmetry potentials. Since the value of Lane potential is very uncertain, in order to make comparisons, we have also investigated the cases when the symmetry potential of hyperons (and also of resonances) is switched off.

### III. CALCULATIONS AND RESULTS

#### A. Pion- and Hyperon-Production without symmetry potential

In the UrQMD model, the total cross section depends on the isospins of colliding particles, their flavour and the center-of-mass energy. If high quality experimental data on the respective cross sections (the neutron-proton, proton-proton elastic scattering cross sections, *etc.*) exist, a phenomenological fit to the respective data is adopted. If no data are available,

the Additive Quark Model (AQM) and the detailed balance arguments are used. The details of the determination of the elementary cross sections can be found in ref. [13].

First of all, we check the pion and  $\Sigma$  hyperon production when the symmetry potential is not taken into account. In the version 1.3 of UrQMD model, compared to the version 1.2, a channel of  $pp \rightarrow pK\Sigma$  is implemented for the improvement of the kaon production at low energies. The introduction of this channel may also influence the yields of hyperons. In Fig. 2, we show the yields of pions,  $\Lambda$ , and  $\Sigma$  hyperons in the reaction  $^{132}\text{Sn} + ^{132}\text{Sn}$  at  $E_b = 2.5A$  GeV and  $b = 2$  fm, calculated by using both the versions 1.2 and 1.3 of UrQMD, and with and without iso-scalar part of the mean field. The EoS0(v1.2) and EoS0(v1.3) denote the results of the versions 1.2 and 1.3 without the mean field, and the EoS1(v1.3) denotes the results of the version 1.3 with a mean field of hard Skyrme-type force. The freeze-out time is taken to be  $30\text{ fm}/c$  and for each case we calculate tens of thousand events for good statistics. In Fig. 2 (lower panel) we find that the effect of introducing the process of  $pp \rightarrow pK\Sigma$  and the mean field on  $\pi$  production is almost negligible, but its effect on the hyperon production is rather large (see upper panels in Fig. 2). The yield of  $\Sigma$  hyperon is enhanced by about 20% whereas the yield of  $\Lambda$  hyperon is suppressed by about 22% with the version 1.3, which together suppresses the  $\Lambda + \Sigma^0$  yields by about 15%. When the mean field is switched on, the suppression effect on the yields of hyperons is enhanced by about 35 – 40%, the same as in [15]. In Refs. [12, 13, 15], it was pointed out that the yields of hyperons within the cascade model were always overestimated. This means that our suppressed yields of the hyperon production, with mean-field correction, could be in the right direction of the experiments at these energies.

In Fig. 3, we show the fractions of the yields of pions and  $\Sigma$  hyperons produced in different baryon density regions, for cases of  $E_b = 1.5A$  and  $3.5A$  GeV. Here the percentage of the contributions in the individual density regions to the total yield is plotted. In general, pions and  $\Sigma$  hyperons are mainly produced in the high density region ( $u > 1$ ). Our calculations at both the energies show that more than 75% of pions and  $\Sigma$  hyperons are produced in the region of  $u > 1$ . Among them, more than 50% is produced in the region of  $u = 1 - 3$ , and the remaining is produced in the region of  $u > 3$ . This happens because the phase-space available at such higher densities is quite restricted. Furthermore, with the energy increasing from  $1.5A$  GeV to  $3.5A$  GeV, the fractions of the yields of  $\pi$  (and  $\Sigma$ ) produced in the density region of  $u = 1 - 3$  decrease while those at other densities increase. Comparing the pion

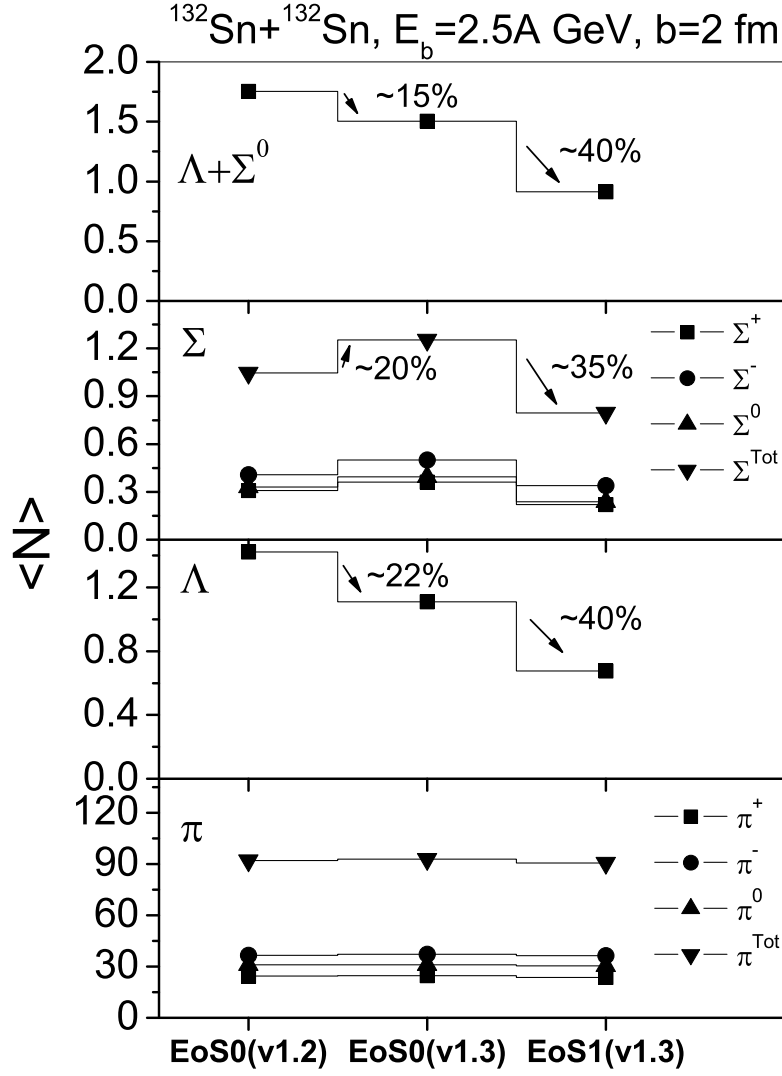


FIG. 2: The  $\pi$ ,  $\Lambda$ ,  $\Sigma$ , and  $(\Lambda + \Sigma^0)$  yields with different conditions in the  $^{132}\text{Sn} + ^{132}\text{Sn}$  reaction at  $E_b = 2.5A$  GeV and impact parameter  $b = 2$  fm. EoS0 and EoS1 refer, respectively, to without and with isoscalar part of the mean field, v1.2 and v1.3 being the version 1.2 and version 1.3 of UrQMD (see text).

and  $\Sigma$  production, we find that at both energies the fraction of pions produced is larger than that of  $\Sigma$  hyperons for densities  $u < 2$ , while the situation is just opposite for densities  $u > 2$ .

Figs. 4 (a) and (b) show the percentage of the contributions from the relevant Baryon-



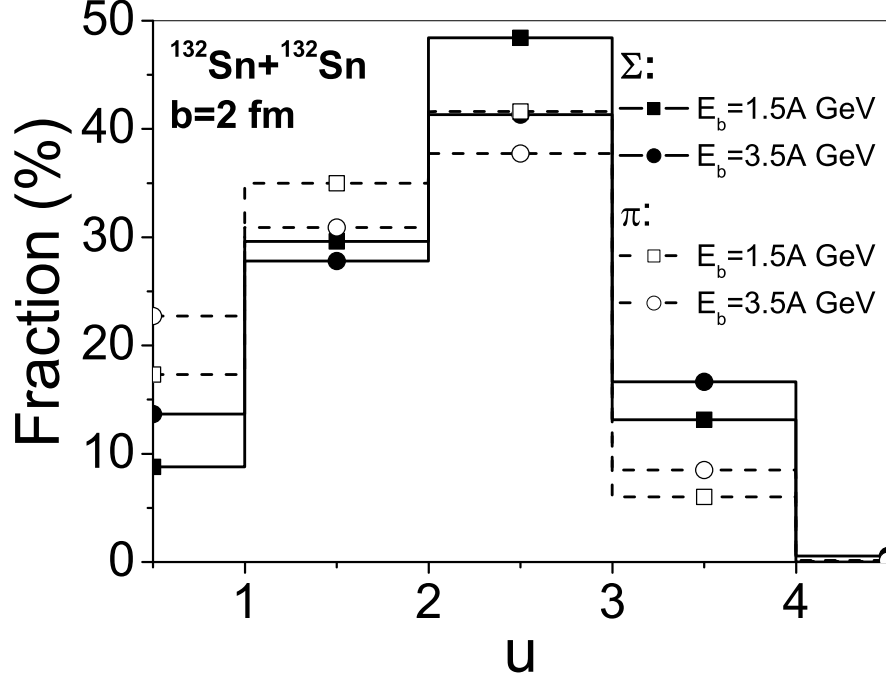


FIG. 3: The production fractions of  $\pi$  and  $\Sigma$  at different densities for  $^{132}\text{Sn} + ^{132}\text{Sn}$  reactions at  $E_b = 1.5A$  and  $3.5A$  GeV and  $b = 2$  fm.

Baryon (B-B), Meson-Baryon (M-B) inelastic scattering, and the resonance (Res) decay processes to the total  $\Sigma$  hyperon production and annihilation at (a)  $E_b = 1.5A$  GeV and (b)  $E_b = 3.5A$  GeV. It should be pointed out that in these results, the contributions from the  $B\Sigma \rightarrow \Sigma X$  in  $BB \rightarrow \Sigma X$  and the  $M\Sigma \rightarrow \Sigma X$  in  $MB \rightarrow \Sigma X$  are added to both the  $\Sigma$  hyperon production and annihilation processes. Here, and below, "X" represents the products (including multi-hadrons) other than  $\Sigma$ . From these two plots, we find that the most important channels for  $\Sigma$  production and annihilation are  $MB \rightarrow \Sigma X$ , and the Res ( $B^* \rightarrow \Sigma X$ , and  $\Sigma M \rightarrow B^*$ ) at the two energies studied.

Figs. 4 (c) and (d) show the time evolution of the average number of  $\Sigma$  produced and annihilated per unit time,  $dN_\Sigma/dt$ , through the processes of  $MB \rightarrow \Sigma X$ ,  $B^* \rightarrow \Sigma X$ , and  $M\Sigma \rightarrow B^*$  at  $E_b = 1.5A$  GeV and  $E_b = 3.5A$  GeV, respectively. Here, the unit time is taken to be  $2fm/c$ . For  $\Sigma$  production, at the early stage, the channel  $MB \rightarrow \Sigma X$  is the most important one. The  $dN_\Sigma/dt$  for  $MB \rightarrow \Sigma X$ , particularly at  $E_b = 3.5A$  GeV, is very much pronounced at the early reaction time, but then it decreases, even faster than for the

case of 1.5A GeV. The  $dN_\Sigma/dt$  for  $MB \rightarrow \Sigma X$  is reduced to  $\sim 20\%$  of its highest value at  $t = 10 fm/c$  for the case of  $E_b = 3.5A$  GeV but at  $t = 12 fm/c$  for the case of  $E_b = 1.5A$  GeV. At the late reaction stage,  $\Sigma$  is mainly produced from the decay of baryon resonances (i.e.  $\Sigma^*$  or  $\Lambda^*$ ), which then continues for a longer time. Concerning the  $dN_\Sigma/dt$ -value for the  $\Sigma$  annihilating channel of  $M\Sigma \rightarrow B^*$ , it is much smaller compared to the case of the reverse process of  $B^* \rightarrow \Sigma X$  at  $E_b = 1.5A$  GeV, while it remains comparable at  $E_b = 3.5A$  GeV. The reason for this behavior is that a larger number of  $\Sigma$ 's are produced through  $MB \rightarrow \Sigma X$  at  $E_b = 3.5A$  GeV than at  $E_b = 1.5A$  GeV, which leads to a stronger annihilation of  $\Sigma$ 's at  $E_b = 3.5A$  GeV. Thus, from Figs. 4 (c) and (d) we may conclude that  $\Sigma$  hyperons are mainly produced during  $t < 10 fm/c$  for the case of  $E_b = 3.5A$  GeV but continues up to  $t \sim 12 fm/c$  for the case of  $E_b = 1.5A$  GeV.

Fig. 5 shows the time evolution of the average density in the central reaction zone of  $|r| < 5 fm$  at  $E_b = 1.5A$  and  $3.5A$  GeV. One sees that the average density in the region of  $|r| < 5 fm$  reduces to the normal density at  $t \sim 12 fm/c$  for the case of  $E_b = 3.5A$  GeV, but for  $E_b = 1.5A$  GeV at  $t \sim 16 fm/c$ . Compared to the case when  $dN_\Sigma/dt$  for the process  $MB \rightarrow \Sigma X$  reduces to  $\sim 20\%$  of its highest value, this result at high energy is similar but is somewhat longer at the lower energy. In other word, Figs. 4 and 5 show that, compared to the time when the system stays at high densities ( $u > 1$ ), the time when most of the  $\Sigma$  hyperons are produced is similar at  $E_b = 3.5A$  GeV but is somewhat *shorter* at  $E_b = 1.5A$  GeV.

Similar to Figs. 4 (a) and (b), Fig. 6 shows the accumulated number of  $\pi$ 's produced and annihilated via the different processes. Unlike  $\Sigma$ , pion is mainly produced via the baryon decay, where the most important process is  $\Delta$  decay. The contribution from other channels, such as  $BB$ ,  $MB$ ,  $M$  decay, as well as  $N^*(1440)$  decay, becomes visible only for the case of 3.5A GeV. The obvious difference between the two cases of  $E_b = 1.5A$  GeV and 3.5A GeV is that the *fraction* of  $\pi$  produced via  $\Delta$  decay is much smaller for the higher energy case. A similar scenario occurs for  $\pi$  annihilation.

## B. The effect of the symmetry potential on $\pi^-/\pi^+$ and $\Sigma^-/\Sigma^+$ ratios

In this section, we mainly explore the effect of the symmetry potential on the ratios between the yields of negatively and positively charged pions and  $\Sigma$  hyperons. In Fig. 7, we

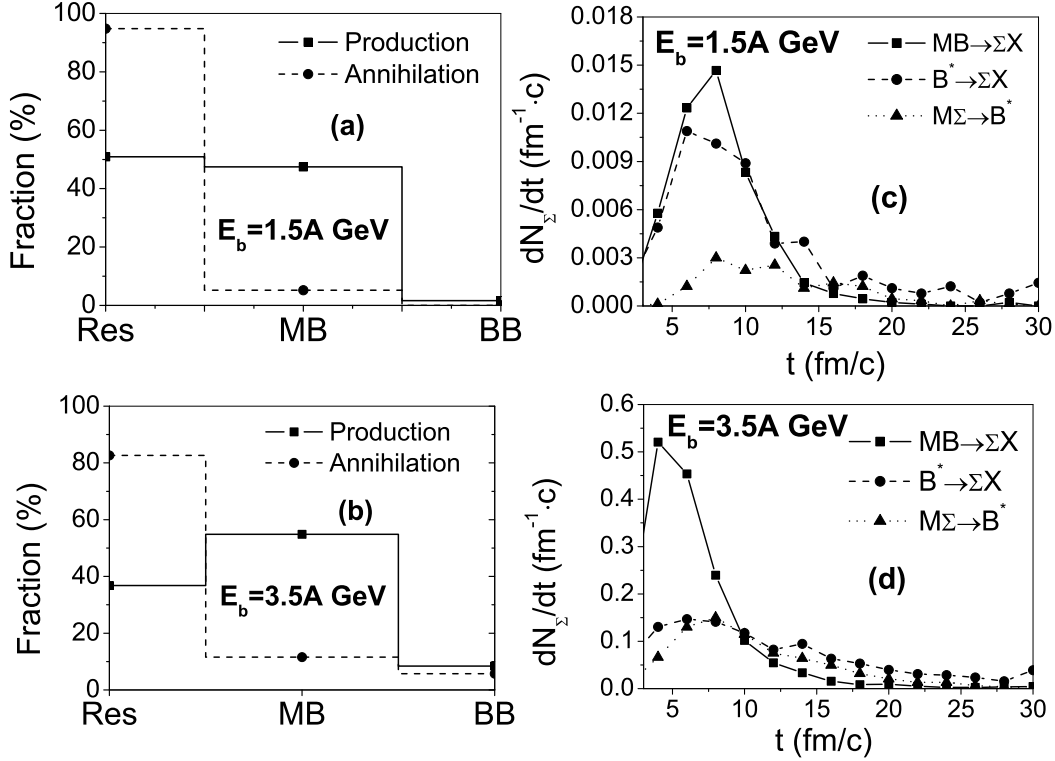


FIG. 4: The contributed ratios of each channel (BB, MB or Res) for  $\Sigma$  production or annihilation plotted at (a)  $E_b = 1.5A$  GeV and (b)  $3.5A$  GeV. The time evolution of  $dN_\Sigma/dt$  of several important  $\Sigma$  production and annihilation processes is shown at (c)  $E_b = 1.5A$  GeV and (d)  $E_b = 3.5A$  GeV.

show the time evolution of the  $\pi^-/\pi^+$  ratios (left-hand side) and the  $\Sigma^-/\Sigma^+$  ratios (right-hand side) calculated with  $F_1^{\gamma=1}$  and  $F_2^{a=3}$  for the reaction  $^{132}\text{Sn} + ^{132}\text{Sn}$  at  $E_b = 1.5A$ ,  $2.5A$ ,  $3.5A$  GeV and  $b = 2$  fm, and  $^{112}\text{Sn} + ^{112}\text{Sn}$  at  $E_b = 3.5A$  GeV and  $b = 2$  fm. The symmetry potentials of all the particles mentioned in Sec. II are considered. Here, and below, the  $\Sigma$  resonances are also included in order to improve the statistics of calculated quantities at the early stage of the reaction. Also, at the freeze-out time, all the unstable particles are considered to decay. For the pions, one can see from the left plot in Fig. 7 that at  $E_b = 1.5A$  GeV the  $\pi^-/\pi^+$  ratio calculated with the soft symmetry potential ( $F_2^{a=3}$ ) is enhanced compared with the stiff one ( $F_1^{\gamma=1}$ ), which is the same as was found in [8]. This happens because, at this energy, pions are mainly produced by  $\Delta$  decay (refer to Fig. 6).

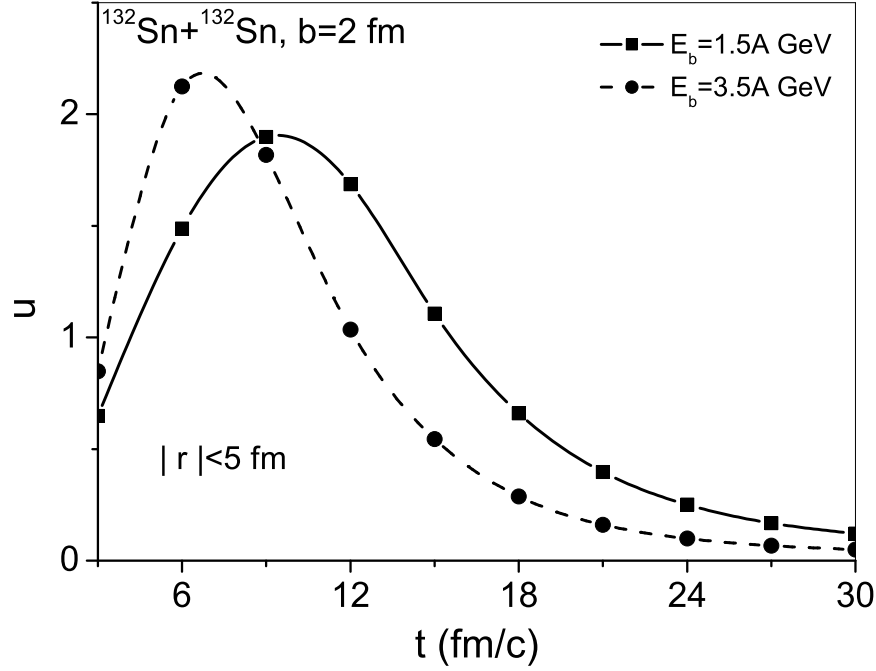


FIG. 5: The time evolution of the average density in central collision zone at  $E_b = 1.5A$  and  $3.5A$  GeV.

Furthermore, we also find that the difference in the ratios of  $\pi^-/\pi^+$  calculated with different symmetry potentials  $F_1^{\gamma=1}$  and  $F_2^{a=3}$  is reduced with the increase of the beam energy, like in Ref. [11]. The reason for this insensitivity at high energies is that more  $\pi$  production and annihilation channels are involved at high energies and then the  $\pi$  production and annihilation via  $\Delta$ -decay also become less important. In [11], it is mentioned that the recent FOPI data show this above noted tendency. Thus, we could take the ratio  $\pi^-/\pi^+$  at high energies (as is the case with  $E_b = 3.5A$  GeV studied in this work) to have become insensitive to the symmetry potential.

Next, for  $\Sigma$  hyperons, from Fig. 7 (right plot), firstly, one sees that the  $\Sigma^-/\Sigma^+$  ratio is sensitive to the density dependence of the symmetry potential for neutron-rich  $^{132}\text{Sn} + ^{132}\text{Sn}$  collisions, but insensitive to that for the nearly symmetric  $^{112}\text{Sn} + ^{112}\text{Sn}$  collisions. For  $^{132}\text{Sn} + ^{132}\text{Sn}$  at  $E_b = 1.5A$  GeV, the  $\Sigma^-/\Sigma^+$  ratio calculated with the stiff symmetry potential is higher than the one with the soft symmetry potential. As the beam energy increases, the  $\Sigma^-/\Sigma^+$  ratio falls and the difference between the  $\Sigma^-/\Sigma^+$  ratios calculated

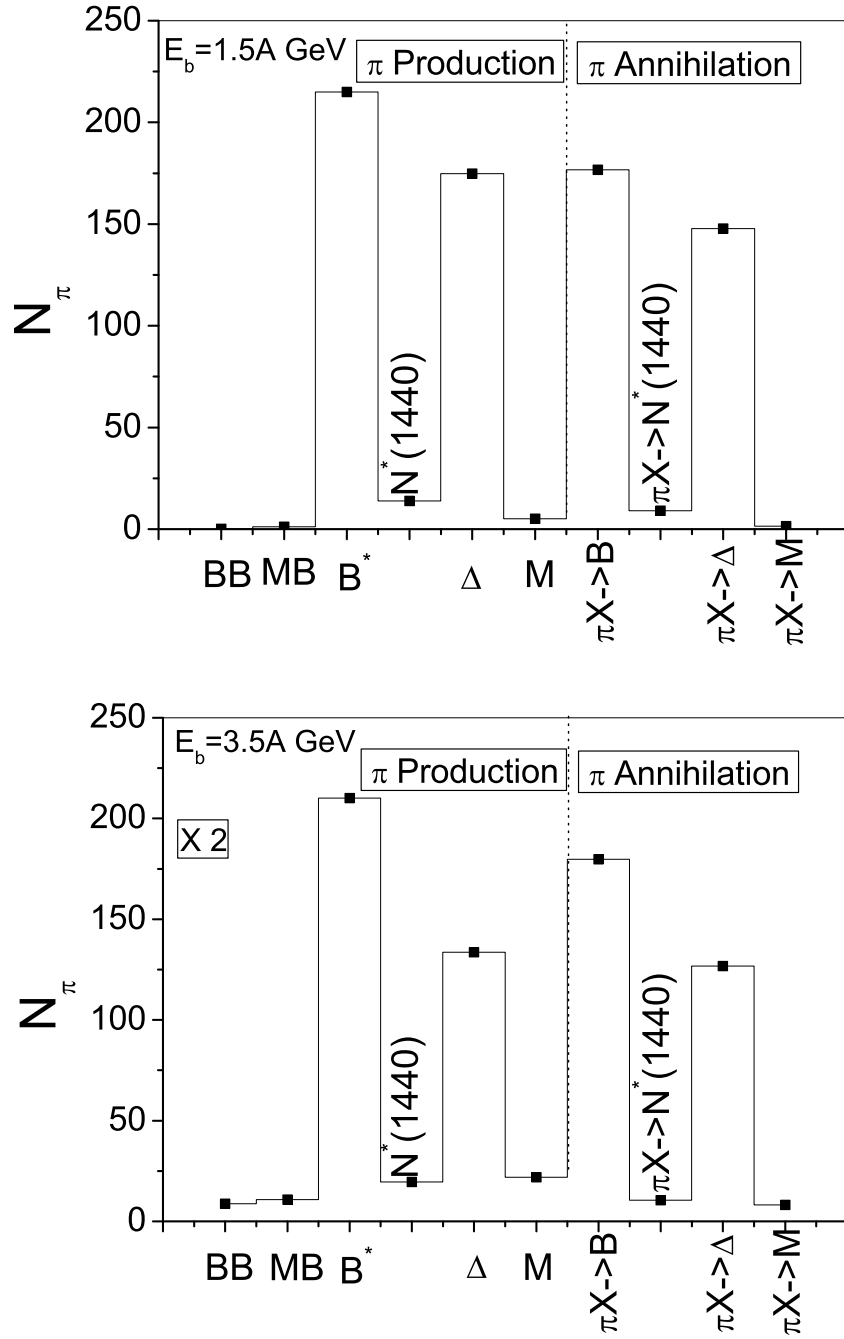


FIG. 6: The average number of  $\pi$  produced and annihilated through different channels for  $^{132}\text{Sn} + ^{132}\text{Sn}$  at  $E_b = 1.5A \text{ GeV}$  (upper plot) and  $3.5A \text{ GeV}$  (lower plot). For a comparison between the two plots, the number in lower plot is drawn as half of the real quantity.

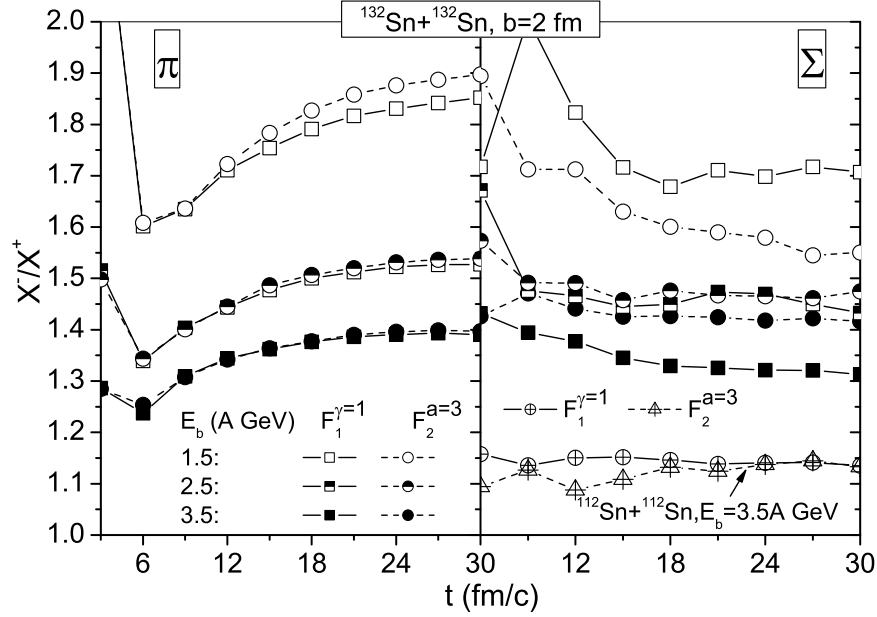


FIG. 7: The ratios  $\pi^-/\pi^+$  (left) and  $\Sigma^-/\Sigma^+$  (right) for the collisions  $^{132}\text{Sn} + ^{132}\text{Sn}$  ( $E_b = 1.5A$ ,  $2.5A$ , and  $3.5A$  GeV;  $b = 2$  fm) and  $^{112}\text{Sn} + ^{112}\text{Sn}$  ( $E_b = 3.5A$  GeV;  $b = 2$  fm), calculated with the different symmetry potentials  $F_1^{\gamma=1}$  and  $F_2^{a=3}$ .

with  $F_1^{\gamma=1}$  and  $F_2^{a=3}$  reduces strongly. As the beam energy increases further, at  $E_b = 3.5A$  GeV the  $\Sigma^-/\Sigma^+$  ratio falls further but the difference between the  $\Sigma^-/\Sigma^+$  ratios calculated with  $F_1^{\gamma=1}$  and  $F_2^{a=3}$  appears again, the  $\Sigma^-/\Sigma^+$  ratio with soft symmetry potential now becoming higher than that with the stiff one.

In sequel, it might be interesting to investigate why the behavior of  $\Sigma^-/\Sigma^+$  and  $\pi^-/\pi^+$  ratios is so different, as far as the influence of the density dependence of the symmetry potential is concerned. One basic difference is that, like nucleons,  $\Sigma^\pm$  hyperons are under the influence of the mean field produced by the surrounding nucleons, as soon as they are produced. The symmetry potential of hyperons also play an important dynamic role and results in a strong effect on the ratio of the negatively to positively charged  $\Sigma$  hyperons. Thus, we further investigate the  $\Sigma^-/\Sigma^+$  and  $\pi^-/\pi^+$  production ratios when the symmetry potential of  $\Sigma$  hyperons and resonances, except nucleons, is switched off. A very small difference for the  $\pi^-/\pi^+$  ratio, but a large difference for  $\Sigma^-/\Sigma^+$  ratio is found with the switching on and off of the symmetry potential of  $\Sigma$  and resonances. Our results for  $\Sigma^-/\Sigma^+$

ratio are plotted in Fig. 8. Two cases are demonstrated: 1) only the symmetry potential of nucleons is considered; and 2) only the  $\Sigma$  symmetry potential is not considered.

From Fig. 8 one sees that the  $\Sigma^-/\Sigma^+$  ratio at  $E_b = 1.5A$  GeV with soft symmetry potential is higher than with the stiff symmetry potential, no matter whether the symmetry potential of  $N^*(1440)$ ,  $\Delta$ , and  $\Lambda$  is introduced or not. As the incident energy is increased to  $3.5A$  GeV, the sensitivity to the density dependence of the symmetry potential is almost lost, like for the case of  $\pi^-/\pi^+$  ratio (not shown here). This means that the different behavior of the  $\Sigma^-/\Sigma^+$  ratio, with respect to the  $\pi^-/\pi^+$  ratio in Figs. 7, is due to the introduction of the symmetry potential of  $\Sigma$  hyperon. This can be understood as follows: In Fig. 4, it was shown that one of the most important channel for  $\Sigma$  production is  $MB \rightarrow \Sigma X$ , where the most important channel is  $\pi N \rightarrow \Sigma X$ . There are primarily 6 processes for  $\pi N \rightarrow \Sigma X$ , namely, 1)  $\pi^+n \rightarrow \Sigma^0 K^+$ , 2)  $\pi^+n \rightarrow \Sigma^+ K^0$ , 3)  $\pi^-n \rightarrow \Sigma^- K^0$ , 4)  $\pi^-p \rightarrow \Sigma^- K^+$ , 5)  $\pi^-p \rightarrow \Sigma^0 K^0$ , 6)  $\pi^+p \rightarrow \Sigma^+ K^+$ . The 1) and 5) are not relevant here; 2) and 6) are relevant to the  $\Sigma^+$  production and 3) and 4) are relevant to the  $\Sigma^-$  production. Thus, one can draw the conclusion that the  $\Sigma^-/\Sigma^+$  ratio should be proportional to the  $\pi^-/\pi^+$  ratio, and hence, the  $\Sigma^-/\Sigma^+$  ratio has the same behavior as the  $\pi^-/\pi^+$  ratio when the symmetry potential of  $\Sigma$  is not taken into account.

#### IV. SUMMARY AND DISCUSSION

In summary, based on the UrQMD model (version 1.3), we have investigated the influence of the symmetry potential on the ratios between the negatively and positively charged pions and  $\Sigma$  hyperons, in the nearly central collisions  $^{132}\text{Sn} + ^{132}\text{Sn}$  and  $^{112}\text{Sn} + ^{112}\text{Sn}$  at  $1.5A$ ,  $2.5A$  and  $3.5A$  GeV energies. In order to find sensitive probes to the behavior of the symmetry potential at high-density nuclear matter, two different forms of the density dependence of symmetry potential in the mean field are considered. The obvious dynamical effect of the symmetry potential is found on the neutron-rich reaction  $^{132}\text{Sn} + ^{132}\text{Sn}$  and not on the nearly isospin-symmetric reaction  $^{112}\text{Sn} + ^{112}\text{Sn}$ . The effect of the symmetry potential on the  $\pi^-/\pi^+$  ratio in  $^{132}\text{Sn} + ^{132}\text{Sn}$  at  $E_b = 1.5A$  GeV is similar to that found in [8, 11], namely, the  $\pi^-/\pi^+$  ratio calculated with the soft symmetry potential is higher than that with the stiff one, but at higher energies, like  $E_b = 3.5A$  GeV, it disappears. This is explained as follows: at  $E_b = 1.5A$  GeV the most important channel for the production of pions is  $\Delta$

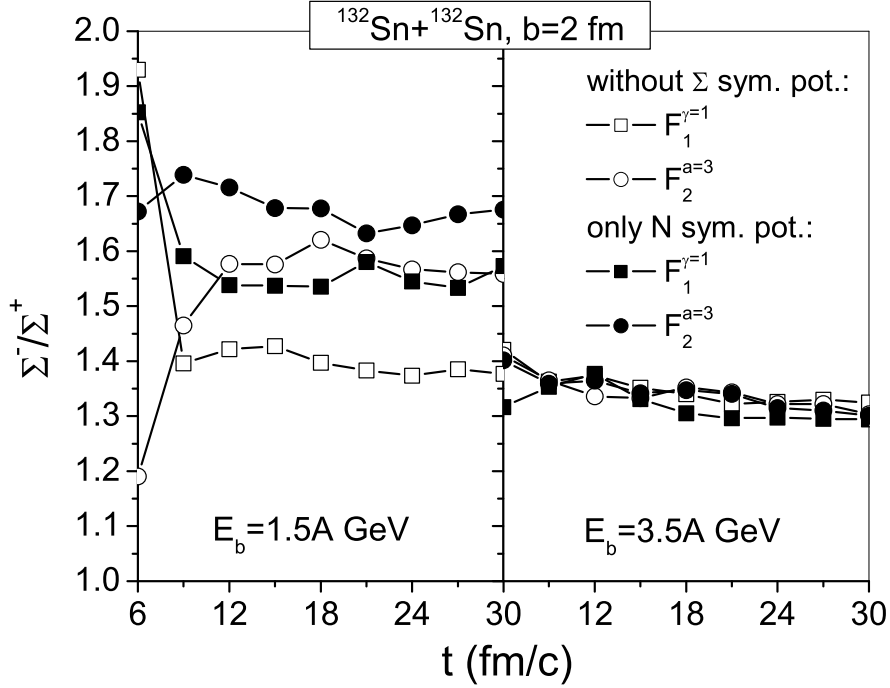


FIG. 8: The ratios  $\Sigma^-/\Sigma^+$  for  $F_1^{\gamma=1}$  and  $F_2^{a=3}$ , with the symmetry potentials of different baryons switched on or off.

decay, while at  $E_b = 3.5A$  GeV other channels also play important role and the contribution from  $\Delta$  decay is largely reduced.

The situation about the effect of the symmetry potential on  $\Sigma^-/\Sigma^+$  is more complicated because  $\Sigma$  hyperon itself also experiences a mean field of nuclear medium as soon as it is produced. When the symmetry potential of  $\Sigma$  hyperons is not taken into account, a behavior similar to that of  $\pi^-/\pi^+$  ratio is obtained, i.e., the  $\Sigma^-/\Sigma^+$  ratio calculated with the soft symmetry potential is higher than that with the stiff one at  $E_b = 1.5A$  GeV and the sensitivity to the symmetry potential disappears at  $E_b = 3.5A$  GeV.

As soon as the symmetry potential of  $\Sigma$  is introduced, the motions of  $\Sigma^-$  and  $\Sigma^+$  are also governed by the symmetry potential, in addition to the iso-scalar part of the single-particle potential. The density dependence of  $\mu^{sym}$  (see Fig. 1, where  $\mu^{sym}$  of  $\Sigma^-$  is similar to that of neutron and that of  $\Sigma^+$  is similar to that of proton) drives  $\Sigma^-$  ( $\Sigma^+$ ) to high (low) density area for soft symmetry potential and to low (high) density area for stiff symmetry potential, when the density is higher than the crossing density, and vice versa when the density is lower than



the crossing density, though the effect is then much smaller. Simultaneously,  $\Sigma^-$  ( $\Sigma^+$ ) with soft symmetry potential possesses lower (higher) symmetry potential energy than that with stiff symmetry potential, when density is higher than the crossing density, and vice versa when density is lower than the crossing density. For the case of  $E_b = 1.5A$  GeV, the time duration at high densities ( $u > 1$ ) is much longer than the time when the most of  $\Sigma$  hyperons are produced. Therefore, the situation in this case is mostly like that of the case when the density is higher than the crossing density, i.e.,  $\Sigma^-$  hyperons move to the high density area and  $\Sigma^+$  hyperons move to the low density area for the soft symmetry potential. Thus, with the soft symmetry potential, the annihilation of  $\Sigma^-$  is enhanced and that of  $\Sigma^+$  is reduced, compared with those with stiff symmetry potential. Furthermore, the single-particle energy of  $\Sigma^-$  with the stiff symmetry potential is higher than that with the soft symmetry potential, which leads to more  $\Sigma^-$  hyperons emitted for the stiff symmetry potential case than for the soft one. Finally, the  $\Sigma^-/\Sigma^+$  ratio with the stiff symmetry potential may exceed the one with that of the soft symmetry potential. On the other hand, for the case of  $E_b = 3.5A$  GeV, the duration time at high density is much shorter, as is also the case for the  $\Sigma$  hyperons produced at high densities. Also, the nuclear density reduces quickly and the most of  $\Sigma$  hyperons after their production will experience the situation with the density being lower than the crossing density. Consequently, the  $\Sigma^-/\Sigma^+$  ratio with the soft symmetry potential may exceed as compared to that with the stiff symmetry potential. This kind of energy dependence of the behavior of the  $\Sigma^-/\Sigma^+$  ratio with respect to the symmetry potential is completely due to the dynamical effect of the symmetry potential of  $\Sigma$  in nuclear medium, which allows us to understand why the behavior of the  $\Sigma^-/\Sigma^+$  ratio is different from the  $\pi^-/\pi^+$  ratio. However, there exists a large uncertainty about the single-particle potential of  $\Sigma$ , especially the symmetry potential, so that the results presented here may not be accurate quantitatively. However, all the features about the energy dependence of the relative values of the  $\Sigma^-/\Sigma^+$  ratios, corresponding to the different forms of the density dependence of the symmetry potential, should not change. These features are also useful for us to extract the information about the symmetry potential of  $\Sigma$  hyperon.

## Acknowledgments

This work is supported by the National Natural Science Foundation of China under Grant Nos. 10175093 and 10235030, Major State Basic Research Development Program under Contract No. G20000774, the Knowledge Innovation Project of the Chinese Academy of Sciences under Grant No. KJCX2-SW-N02, the CASK.C. Wong Post-doctors Research Award Fund, and the Alexander von Humboldt Foundation, Germany.

---

- [1] B.A. Li, *et al.*, Int. J. Phys. **E7**, 147 (1998).
- [2] B. Alex Brown, Phys. Rev. Lett. **85**, 5296 (2000).
- [3] J. Margueron, J. Navarro, N. Van Giai, and W. Jiang, nucl-th/0110026.
- [4] C.M. Ko and G.Q. Li, J. Phys. **G22**, 225 (1996).
- [5] G.Q. Li, C.H. Lee, and G.E. Brown, Nucl. Phys. A **625**, 372 (1997).
- [6] W. Cassing, *et al.*, Phys. Rep. **308**, 65 (1999).
- [7] C. Fuchs, Prog. Part. Nucl. Phys. **53** 113 (2004).
- [8] B.A. Li, Phys. Rev. Lett. **88**, 192701 (2002).
- [9] B.A. Li, Nucl. Phys. A **722**, 209 (2003).
- [10] T. Gaitanos, M. Di Toro, G. Ferini, M. Colonna, and H.H. Wolter, nucl-th/0402041.
- [11] T. Gaitanos, M. Di Toro, S. Typel, V. Baran, C. Fuchs, V. Greco, and H.H. Wolter, Nucl. Phys. A **732** 24 (2004).

- [12] S.A. Bass, *et al.*, Prog. Part. Nucl. Phys. **41**, 225 (1998).
- [13] M. Bleicher, *et al.*, J. Phys. G: Nucl. Part. Phys. **25**, 1859 (1999).
- [14] H. Weber, E.L. Bratkovskaya, W. Cassing, and H. Stöcker, Phys. Rev. C **67**, 014904 (2003).
- [15] M. Reiter, E.L. Bratkovskaya, M. Bleicher, W. Bauer, W. Cassing, H. Weber, and H. Stöcker, Nucl. Phys. A **722**, 142 (2003).
- [16] A.M. Lane, Nucl. Phys. A **128**, 256 (1969).
- [17] J. Dabrowski, Phys. Rev. C **60**, 025205 (1999).
- [18] A. Gal and D.J. Millener, Phys. Lett. B **138**, 337 (1984).
- [19] T. Harada, S. Shinmura, Y. Akaishi, and H. Tanaka, Nucl. Phys. A **507**, 715 (1990).
- [20] N.K. Glendenning and S.A. Moszkowski, Phys. Rev. Lett. **67**, 2414 (1991).
- [21] J. Schaffner and I.N. Mishustin, Phys. Rev. C **53**, 1416 (1996).